# Filter Flexibility and Distortion in a Bacterial Inward Rectifier $K^+$ Channel: Simulation Studies of KirBac1.1

Carmen Domene,*† Alessandro Grottesi,* and Mark S. P. Sansom*
*Laboratory of Molecular Biophysics, Department of Biochemistry, University of Oxford, Oxford, OX1 3QU United Kingdom; and
†Physical and Theoretical Chemistry Laboratory, Department of Chemistry, University of Oxford, Oxford, OX1 3QZ United Kingdom

ABSTRACT The bacterial channel KirBac1.1 provides a structural homolog of mammalian inward rectifier potassium (Kir) channels. The conformational dynamics of the selectivity filter of Kir channels are of some interest in the context of possible permeation and gating mechanisms for this channel. Molecular dynamics simulations of KirBac have been performed on a 10-ns timescale, i.e., comparable to that of ion permeation. The results of five simulations (total simulation time 50 ns) based on three different initial ion configurations and two different model membranes are reported. These simulation data provide evidence for limited (<0.1 nm) filter flexibility during the concerted motion of ions and water molecules within the filter, such local changes in conformation occurring on an ~1-ns timescale. In the absence of $K^+$ ions, the KirBac selectivity filter undergoes more substantial distortions. These resemble those seen in comparable simulations of other channels (e.g., KcsA and KcsA-based homology models) and are likely to lead to functional closure of the channel. This suggests filter distortions may provide a mechanism of K-channel gating in addition to changes in the hydrophobic gate formed at the intracellular crossing point of the M2 helices. The simulation data also provide evidence for interactions of the "slide" (pre-M1) helix of KirBac with phospholipid headgroups.

## INTRODUCTION

Membrane proteins are of some biological importance, as they account for ~25% of genes. Although traditionally difficult to study using the methods of structural biology, recent advances in protein crystallography, electron microscopy, and NMR are yielding an increasing number of membrane protein structures (see http://blanco.biomol.uci.edu/Membrane_Proteins_xtal.html for a summary). However, such methods yield static, average structures. To fully comprehend the relationship between membrane protein structure and function we need to characterize the conformational dynamics of these proteins. The potassium channels (Yellen, 2002) provide a good test system about which to develop approaches for studying conformational dynamics, as there is a large body of structural and functional data available for this particular class of membrane proteins.

K channels are also of physiological and biomedical interest. They are a ubiquitous family of integral membrane proteins, whose role is the regulation of $K^+$-ion flux across cell membranes. K-channel regulation is accomplished by a conformational change that allows the protein to switch between two alternative (closed versus open) conformations, a process known as ''gating''. Gating is thus an inherently dynamic process that cannot be fully characterized by static structures alone.

The elucidation of the structures of several K channels (Mackinnon, 2003) has shed considerable light on the structural basis of the mechanisms of ion selectivity and permeation (Doyle et al., 1998; Morais-Cabral et al., 2001; Zhou et al., 2001; Jiang et al., 2002a,b, 2003; Kuo et al., 2003). All of these structures are for bacterial K channels. They have differences in their structures corresponding to their different gating mechanism: KcsA, gated by low pH; MthK, gated by $Ca^{2+}$ ions; KvAP, gated by transmembrane (TM) voltage; and KirBac, gating mechanism unknown. However, they all share a core pore-forming domain. This is tetrameric, with the monomers surrounding a central pore. The domain is formed of a M1-P-F-M2 motif, where M1 and M2 are transmembrane helices, and the short P-helix and extended filter (F) region form a reentrant loop between the two TM helices. The selectivity filter is the structural element mainly responsible for the selective conduction of $K^+$ ions. Based on multiple sequence alignments and extensive mutagenesis studies it has been shown that the selectivity for potassium ions is associated with a conserved sequence motif TVGYG (for a recent review see Sansom et al., 2002).

Inward rectifier (Kir) channels have two main physiological roles: they regulate cell excitability by stabilizing the membrane potential close to the K-equilibrium potential, and they are involved in K-transport across membranes (Nichols and Lopatin, 1997; Reimann and Ashcroft, 1999). For example, Kir3.1/Kir3.4 channels modulate cardiac electrical activity, and Kir6.2 is involved in insulin release from pancreatic $\beta$-cells. Two recent structures, of the intracellular domain of mammalian Kir (GIRK1; Nishida and MacKinnon, 2002) and of a complete bacterial Kir homolog (KirBac1.1; Kuo et al., 2003), open up the prospect of a detailed understanding of structure/function relationships in this important family of K channels.

*Submitted January 11, 2004, and accepted for publication March 24, 2004.*
Carmen Domene and Alessandro Grottesi contributed equally to this work.
Address reprint requests to Mark S. P. Sansom, Tel.: 44-1865-275371; Fax: 44-1865-275182; E-mail: mark.sansom@biop.ox.ac.uk.

0006-3495/04/07/256/12 $2.00
doi: 10.1529/biophysj.104.039917

KirBac is the first bacterial Kir whose structure has been solved at 3.65-Å resolution (Kuo et al., 2003). The overall TM topology is similar to that of the simple bacterial channel KcsA, with the addition of a ''slide'' helix N-terminal to the M1 TM helix. However, unlike KcsA, the crystal structure of KirBac reveals an intracellular domain consisting mostly of $\beta$-sheet. This latter domain has a similar fold to the GIRK1 intracellular domain. The KirBac channel is thought to be in a closed (i.e., nonconducting conformation) as the intracellular pore mouth, formed by the crossing point of the C-termini of the M2 helices, is hydrophobic and very narrow (only ~0.05 nm in radius, compared with the 0.133-nm radius of a $K^+$ ion). The selectivity filter of KirBac is quite similar to that of KcsA (see below for a more detailed discussion), with a succession of five potential $K^+$-ion binding sites formed by cages of eight oxygen atoms.

There is considerable interest in the conformational dynamics of the filter of Kir channels (see Bichet et al., 2003 for a recent review). In particular it has been suggested that, in addition to the intracellular gate at the crossing point of the M2 helices, there may also be a component of gating at the selectivity filter. This is not restricted to Kir channels: the phenomenon of C-type inactivation of voltage-gated (Kv) channels is also thought to involve changes in conformation of the selectivity filter. Furthermore, in the absence of $K^+$ ions many K channels seem to enter a ''defunct'' state via changes in the selectivity filter. It is therefore of some interest to characterize the conformational dynamics of the filter region of KirBac and to compare with the experimental and computational behavior of other K channels.

Computational approaches, based on simulations of channel proteins and their permeant ions, allow us to bridge the divide between static structure and dynamic function of ion channels (Roux et al., 2000; Chung and Kuyucak, 2002; Roux, 2002; Giorgetti and Carloni, 2003; Sansom et al., 2000; Tieleman et al., 2001b; Domene et al., 2003a; Compoint et al., 2004) and related membrane proteins. In particular, molecular dynamics (MD) simulations enable us to model the nanosecond timescale dynamics of channels embedded in an atomistic model of a cell membrane. MD simulations have been applied to a range of ion channels, including KcsA (Guidoni et al., 1999, 2000; Guidoni and Carloni, 2002; Bernèche and Roux, 2000, 2001a, 2003; Allen et al., 1999, 2000; Allen and Chung, 2001; Mashl et al., 2001; Åqvist and Luzhkov, 2000; Luzhkov and Åqvist, 2000, 2001; Jordan, 2000; Shrivastava and Sansom, 2000, 2002; Capener et al., 2000; Ranatunga et al., 2001a,b; Biggin et al., 2001; Sansom et al., 2000, 2002; Tieleman et al., 2001b; Capener and Sansom, 2002), and to related channel-like proteins such as the aquaporins (de Groot and Grubmuller, 2001; Zhu et al., 2001; Jensen et al., 2001; Tajkhorshid et al., 2002). Simulation studies of KcsA have provided information on the conformational dynamics of the selectivity filter and on the dynamics and energetics of ion permeation.

In this study we use MD simulations to explore the filter dynamics of KirBac on a timescale (10 ns) comparable to the mean passage time of $K^+$ ion through a channel. To effectively explore the dynamics under different conditions, we have conducted five simulations, corresponding to 50 ns total simulation time, using three different initial ion configurations and two different model membranes. The results of these simulations indicate the importance of filter flexibility in ion permeation. Comparison of these results with those of other simulations and with structural data suggests possible roles of filter distortion in $K^+$-channel gating.

## METHODS

### Simulation system

The coordinates were taken from Protein Data Bank (PDB) entry 1P7B (www.rcsb.org). The transmembrane domain was defined as extending from residue 40–153. The C-terminal carboxylate was protonated and the N-terminal amine unprotonated to form neutral termini. The program Whatif (Vriend, 1990) was used to perform $pK_A$ calculations to aid in assignment of side-chain ionization states, and on the basis of these calculations the side chains of Asp-115 and Glu-130 were protonated. Thus there is a shared proton between Asp-115 and Glu-106, homologous to that shared between Asp-80 and Glu-71 in KcsA (Ranatunga et al., 2001a). The rest of the residues remained in their default ionization state.

### Simulation setup

The systems were solvated with SPC water molecules (Berendsen et al., 1981) retaining all the crystallographic waters. The central cavity (which is somewhat smaller than that of KcsA and does not appear to contain a binding site for a $K^+$ ion in the x-ray structure) was solvated by: i), retaining all the pore water molecules present in the x-ray structure, and ii), overlaying SPC water molecules after the solvation of the entire system. A water molecule was placed at the ''back'' of the selectivity filter, between the pair Glu-106–Asp-115 to mimic the equivalent water in KcsA. The initial $K^+$-ion configuration is detailed below. An ionic strength of 150 mM was used and counterions were added where needed to keep all systems electrically neutral.

Simulations were performed using minor modifications of methods previously employed for KcsA (Domene and Sansom, 2003) and for a homology model of Kir6.2 (Capener and Sansom, 2002). For the simulations in a lipid bilayer the protein was positioned in a preequilibrated 1-palmitoyl-2-oleoyl-phosphatidyl choline (POPC) bilayer so as to maximize possible interaction of the POPC headgroups and the ''belts'' (see below) of amphipathic aromatic side chains on the protein surface. For the membrane-mimetic octane slab simulations a slab of thickness 3.2 nm was used. The final systems contained ~14,000 water molecules plus either 662 octane molecules or 208 POPC molecules, giving totals of ~55,000 atoms.

Once the protein was inserted in the bilayer or surrounded by octane, an equilibration was performed during which the protein atoms were restrained for 0.2 ns. The restraints were then removed and production simulations of 10 ns of duration followed.

### Simulation protocol

MD simulations were performed with GROMACS 3.1.4 (Lindahl et al., 2001) (www.gromacs.org) with a modified version of the GROMOS-87 force field (van Gunsteren and Berendsen, 1987). Lipid parameters were

based on those by Berger et al. (1997) and Marrink et al. (1998). The lipid-protein interactions used GROMOS parameters. Parameters derived from those of Åqvist (1990) were used for the $K^+$ ions.

Simulations were carried out in the NPT ensemble, with periodic boundary conditions. The initial velocities were taken randomly from a Maxwellian distribution at 300 K. The temperature was held constant by coupling to an external bath (Hoover, 1985). Long-range electrostatic interactions were calculated using the particle mesh Ewald summation methods (Darden et al., 1993). Lennard-Jones interactions were calculated using a cutoff of 0.9 nm. The pair lists were updated every 10 steps. The LINCS algorithm (Hess et al., 1997) was used to constrain bond lengths. The timestep was 2 fs, and coordinates were saved every 0.1 ps.

Secondary structure content was calculated using DSSP (Kabsch and Sander, 1983). Other analyses were performed using GROMACS and/or local code. Molecular graphics images were prepared using VMD (Humphrey et al., 1996).

## RESULTS

### Simulation systems

The structure of KirBac is shown in Fig. 1 *A*. As can be seen the molecule is composed of distinct TM and intracellular domains. To focus on events at the filter, and to facilitate comparison with simulations of KcsA (for which the structure of the C-terminal domain has not been determined at high resolution) it was decided to focus simulation studies on the TM domain only. Thus all simulations were for residues 40–153, the N-terminal residues being absent from the crystal structure. Note that the slide helix runs from residues 47–57.

Two models of a membrane were used for the simulations (see Table 1), an explicit lipid bilayer and a bilayer-mimetic octane slab. In simulations PC1–PC3 a lipid bilayer made up of 208 POPC molecules was used, as in previous simulations of K channels. From previous simulations of, e.g., KcsA (Domene et al., 2003b) we have shown that lipid/protein interactions fluctuate on an ~2–5-ns timescale. Thus, we can expect that 10 ns should be long enough for any major changes in KirBac/POPC interactions to relax. However, it is likely that the high viscosity of POPC may be such as to restrict the motions of the protein observable in a time-scale directly addressable by simulations. To overcome this possible restriction we have also performed a couple of simulations in which the POPC bilayer was replaced by a slab of octane molecules. An octane slab has a considerably lower viscosity than POPC, and so might be expected to be more permissive of possible protein conformational changes, but is a reasonable approximation to a lipid bilayer, as demonstrated in a number of previous simulation studies (Tieleman et al., 2001a; Capener and Sansom, 2002).

The density profiles for simulations Oct1 and PC1 are shown in Fig. 2. It can be seen that the octane slab is ~2.8-nm thick whereas the POPC bilayer is ~4.0-nm thick. This difference reflects the absence of the lipid headgroups in the former system. Thus, one of the major differences between the two sets of simulations is the environment experienced by the slide helices (discussed in more detail below).

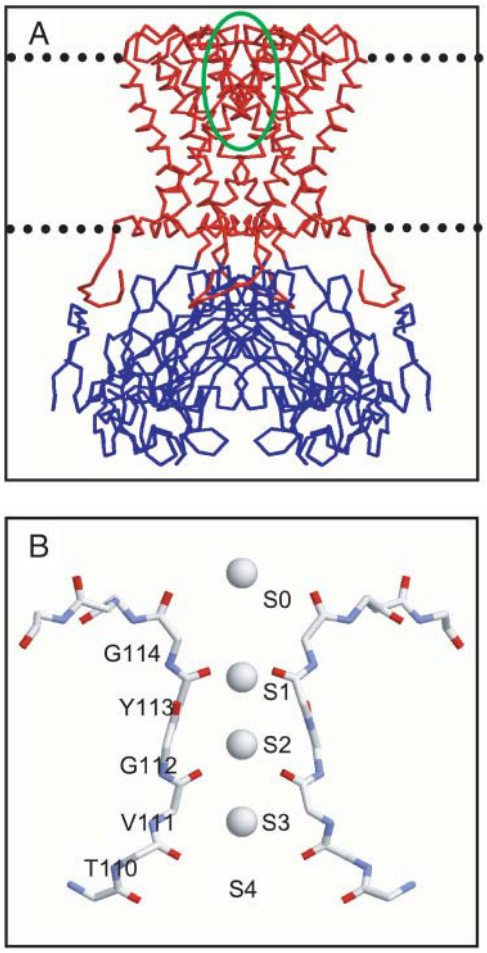


FIGURE 1 (*A*) Structure of KirBac, with the TM domain (residues 40–155) in red and the C-terminal intracellular domain (residues 152–309) in blue. All four subunits are included. The green ellipse indicates the location of the selectivity filter and the horizontal dotted lines indicate the approximate location of the lipid headgroups of a membrane. (*B*) Structure of the selectivity filter (residues 110–114) showing just two subunits for clarity. The four $K^+$ ions observed in the crystal structure (at sites S0, S1, S2, and S3) are shown.

The filter is shown in more detail in Fig. 1 *B*. In the crystal $K^+$ ions are located at sites S1, S2, S3, and in between the $S_{EXT}$ and S0 sites. Of course, the crystal structure is an average (spatial and temporal) and it is not envisaged that all four sites are occupied simultaneously by $K^+$ ions. Note that no ion is observed at site S4 in the crystal structure. To explore the behavior of the selectivity filter as a function of initial ion configuration, two possible arrangements of ions were considered (see Table 1). In simulations Oct1 and PC1 $K^+$ ions were present in sites S1 and S3; in Oct2 the initial sites occupied were $S_{EXT}$ and S2; in PC2 a single $K^+$ ion was present at site S2. In all of the simulations the central cavity accommodated ~28 water molecules but a $K^+$ ion was not present as no such ion is seen in the KirBac x-ray structure (see Fig. 2 *A*).

**TABLE 1 Summary of simulations**

| Simulation | Membrane | $K^+$ ions | Cα RMSD* (nm) | | | | |
|---|---|---|---|---|---|---|---|
| | | | All residues | TM-helix residues | Filter residues | Slide helices | Tail residues |
| Oct1 | Octane | S1 & S3 | 0.53 | 0.17 | 0.09 | 0.26 | 0.99 |
| Oct2 | Octane | $S_{EXT}$ & S2 | 0.54 | 0.16 | 0.11 | 0.34 | 0.94 |
| PC1 | POPC | S1 & S3 | 0.30 | 0.15 | 0.09 | 0.25 | 0.43 |
| PC2 | POPC | S2 | 0.31 | 0.14 | 0.09 | 0.21 | 0.57 |
| PC3 | POPC | No ions | 0.36 | 0.17 | 0.20 | 0.30 | 0.64 |

All simulations were of 10-ns duration.

*The Cα RMSD from the initial conformation was averaged over the final 9 ns of each simulation. The TM-helix residues are defined as M1 (60–82), P (97–109), and M2 (120–150); the filter residues are 110–114; the tails are defined as residues 40–46; and the slide helices are 47–57.

## Conformational stability and fluctuations

Before proceeding with more detailed analysis, it is important to assess the degree of conformational drift in the various simulations. In particular, we wished to evaluate any differences between the two membrane models employed. To this end we analyzed the Cα root-mean-square deviation (RMSD) from the initial structure as a function of time for each simulation (data not shown). In each case the major rise in Cα RMSD seemed to be over within ~1 ns, suggesting that 10 ns is sufficient simulation time. All subsequent analyses were therefore performed in the latter 9 ns of each simulation.

A more detailed analysis of the Cα RMSD values (see Table 1) reveals that, as anticipated, the RMSD values are higher in the octane simulations than in the POPC simulations. It is noteworthy that the ''tail'' regions (i.e., the peptide chain N-terminal to the slide helix; see Table 1 for definitions) have quite high RMSDs. Indeed, if one calculates the Cα RMSDs for the TM helices then values comparable to those seen in simulations of KcsA (Domene and Sansom, 2003; Holyoake et al., 2003) are obtained. The RMSDs for the filter regions are low (~0.1 nm) in all of the simulations (except for PC3 with no $K^+$ ions; discussed in more detail below). Thus, the isolated TM domain of KirBac seems to behave stably in 10-ns simulations and can be used as the basis of further analysis.

Fluctuations in structure as a function of region within the KirBac can be evaluated in terms of the Cα root-mean-square fluctuations (RMSF) as a function of residue number (Fig. 3). For the core TM helices (M1, P, and M2) the Cα RMSFs are <0.1 nm, and in general are a little lower for PC2 than for Oct2. Secondary structure analysis (using DSSP (Kabsch and Sander, 1983); data not shown) confirmed that the M1-P-M2 core region remained unchanged all over the full duration of all the simulations (data not shown). The slide helices (residues 47–57) exhibited greater fluctuations (and RMSDs; Table 1) than the other helices in the molecule. This may reflect two factors: i), the absence of the intracellular domain; and/or ii), interactions of the slide helix with a fluctuating interface between water and membrane. In both simulations the RMSF is quite low in the filter region (residues 110–114), but shows a gradient from the bottom (i.e., residue 110) to the top (i.e., residue 114) of the filter. Details of filter flexibility are discussed below.

## Lipid/protein Interactions

To characterize the behavior of the slide helix in a little more detail for the PC simulations, we have calculated the number of interactions between amphipathic aromatic (Trp, Tyr) residues and lipid headgroups (Fig. 4). A number of studies have indicated the importance of such interactions in stabilizing membrane proteins within lipid bilayers (Yau et al., 1998; Killian and von Heijne, 2000; Killian, 2003). As in previous analysis of such interactions in KcsA simulations (Domene et al., 2003b) there are two bands of interactions. From examination of the structure of KirBac alongside the results of the interaction analysis it is evident that the slide helix makes a major contribution to interactions with lipid headgroups. Of course, these interactions may be modulated by the presence of the intracellular domain, not present in these simulations.

## Ion/filter interactions

A number of experimental, e.g., Morais-Cabral et al. (2001) and computational (Bernèche and Roux, 2000, 2001b, 2003; Guidoni et al., 1999, 2000; Åqvist and Luzhkov, 2000; Shrivastava and Sansom, 2000; Shrivastava et al., 2002; Domene and Sansom, 2003) studies of KcsA indicate that fast ion permeation through the filter occurs via concerted translocations of ions and water molecules between adjacent sites, i.e., $K^+$-ion occupancy of the filter alternates between S0-S2-S4 and S1-S3. Given the high degree of sequence and structural conservation of the filter region between different K channels, one would expect to see similar concerted translocation (on an ~1-ns timescale) in simulations of both KcsA and KirBac. However, this needs to be tested, especially given the suggestions of different (equilibrium) distributions of $K^+$ ions to sites between the KcsA (Morais-Cabral et al., 2001; Zhou et al., 2001) and KirBac (Kuo et al., 2003) crystal structures. To this end, simulations with two

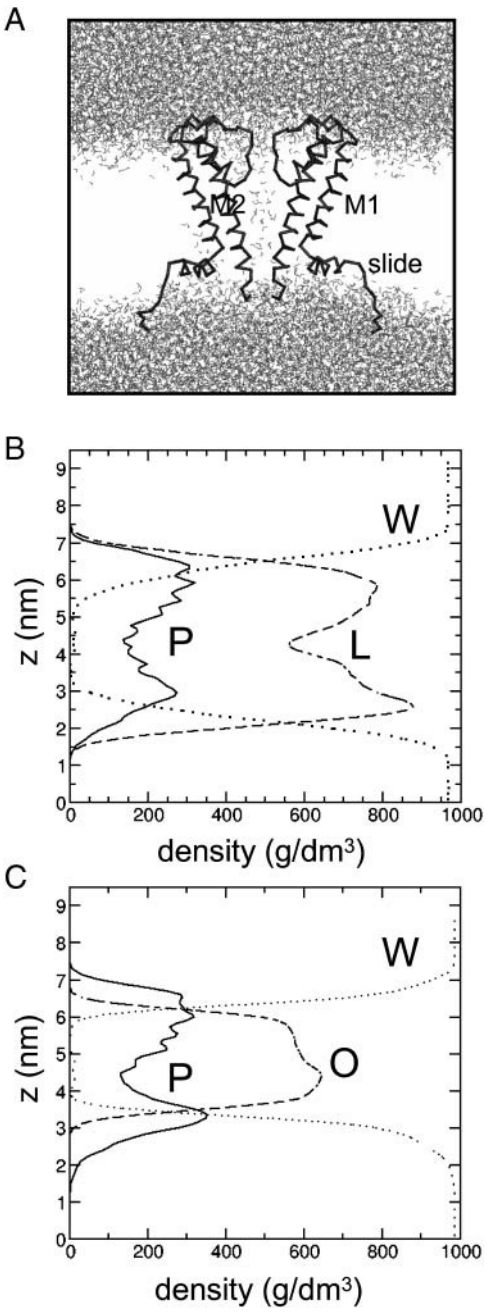


FIGURE 2 (*A*) Schematic representation of the KirBac/POPC simulation system. The C$\alpha$ trace of two subunits and the water molecules are shown; the lipid molecules are omitted for clarity. (*B*, *C*) Component density profiles for simulations (*B*) PC1 and (*C*) Oct1. In both cases the average density over 9 ns is shown as a function of position along the *z* axis (i.e., along the membrane normal) for the protein (*solid line*, *P*), lipid or octane (*dashed line*, *L* or *O*), and water (*dotted lines*, *W*).

different initial $K^+$-ion configurations within the filter were run for each system.

In simulation Oct1 (Fig. 5 *A*) a concerted transition is seen whereby the $K^+$-ion occupancy of the filter switches from S1, S3–S2, S4 after ~0.2 ns, and then remains constant for the rest of the simulation. In simulation Oct2 (Fig. 5 *B*), the

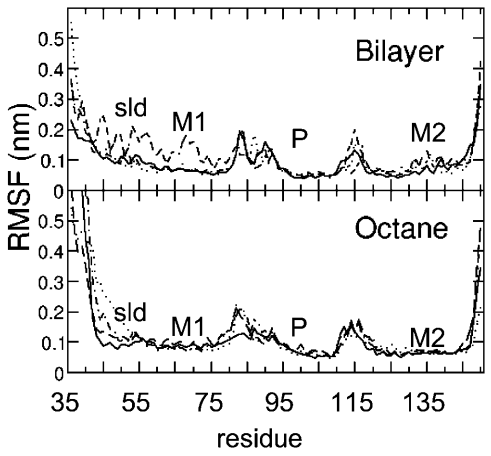


FIGURE 3 C$\alpha$ RMSFs as a function of residue number for the PC1 and Oct1 simulations. In each case the four line styles correspond to the four subunits: M1, M1 helix; M2, M2 helix; P, P helix; sld, slide helix.

initial configuration is $S_{EXT}$, S2. After ~0.3 ns the external ion is partially dehydrated and enters site S0. The configuration remains as S0, S2 for the rest of the simulation. In PC1 a similar behavior to that in Oct1 is observed (Fig. 5 *C*). In PC2 the behavior is similar to that in Oct2 in that the ion at site S2 remains there for the duration of the simulation. Thus it would seem that rapid (<1 ns) concerted transitions of $K^+$-water-$K^+$ between adjacent sites occur in KirBac in much the same manner as for KcsA. On the basis of the four simulations reported here, one is tempted to say that site S2 is particularly favorable for $K^+$ ions in the filter of KirBac. However, more extensive simulations and detailed energetic analysis would be required to be certain of this. It is noteworthy that ions are able to occupy the S4 site even though $K^+$ was not observed at this site in the crystal. Perhaps more details of ion binding would be revealed by a higher resolution structure for KirBac (as was the case for KcsA).

## Filter flexibility

In simulations of KcsA some degree of filter flexibility has been observed (Bernèche and Roux, 2000, 2001b; Shrivastava and Sansom, 2000; Shrivastava et al., 2002; Domene and Sansom, 2003), corresponding mainly to peptide carbonyls flipping in/out from being directed toward the center of the pore. It noteworthy that in the x-ray structure of KirBac, the carbonyl oxygens (COs) of residue G112 do not point directly toward the center of the pore, in contrast with the situation in the KcsA crystal structure. Furthermore, the differences in P-helix conformation and sequence between KirBac and KcsA and difference in the conformation of the tyrosine side chains of the GYG motif mean that the H-bond from the GYG tyrosine of the filter to a tryptophan in the P-helix that seems to stabilize the filter in KcsA (Doyle et al., 1998) is absent from KirBac. It is therefore of some

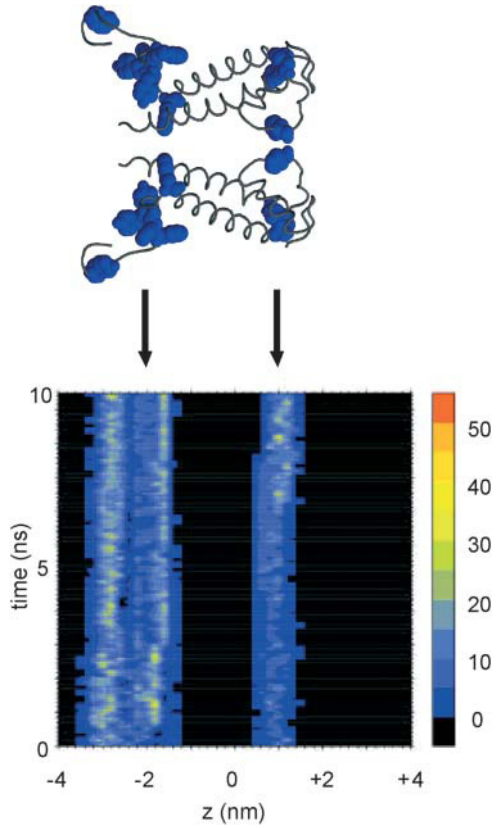


FIGURE 4 Interactions of the amphipathic aromatic (i.e., Tyr, Trp) residues of KirBac with lipid polar headgroups. The upper diagram shows two KirBac TM monomers (oriented with their intracellular ends on the left-hand side) with their Tyr and Trp residues represented in space-filling mode. The lower diagram shows the number of interactions (≤3.5 Å) between these residues and lipid headgroups, shown as a function of position along the bilayer normal ($z$) and time for simulation PC1.

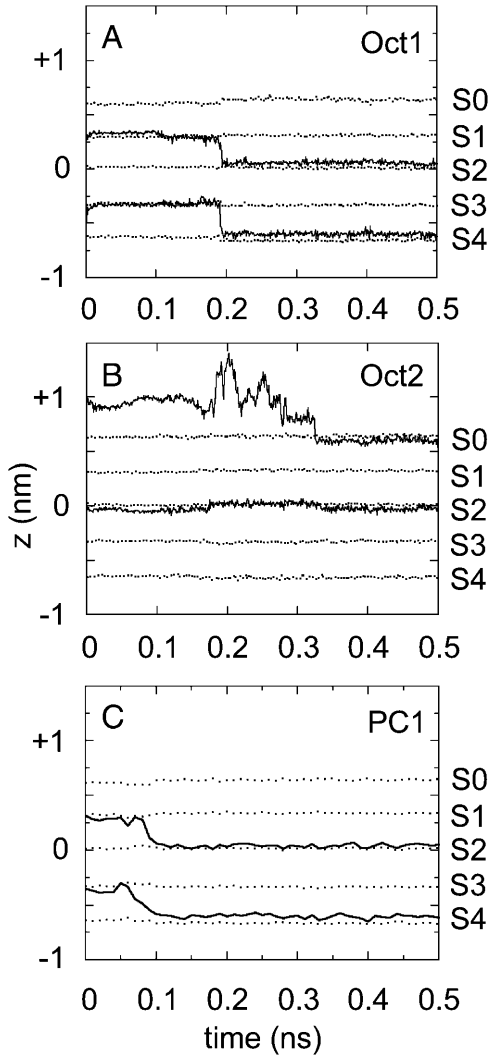


FIGURE 5 Trajectories (for the initial 0.5 ns) of potassium ions in the selectivity filter of KirBac in simulations: (*A*) Oct1, (*B*) Oct2, and (*C*) PC1. In each case the $K^+$-ion positions (*solid lines*) are projected onto the $z$ axis (i.e., the pore axis) and normalized such that the center of the filter has a coordinate of $z = 0$. The positions of the centers of sites S0–S4 are shown as dotted horizontal lines.

interest to characterize in more detail the local flexibility of the filter in KirBac and changes in its conformation during the course of the simulations.

As a measure of the flexibility of the filter we monitored changes with respect to time in the distance between opposing carbonyl oxygens facing one another across the filter. In Fig. 6 we show a change in orientation of the carbonyls of G112 from the initial (crystal) conformation in which the carbonyls point away from the center of the pore to a conformation (more like that of KcsA) in which the carbonyls point toward the center of the pore. This amounts to a change in CO ← → OC separation of the order of 0.2 nm, i.e., each oxygen atom moves by ~0.1 nm. This occurs early on in the simulation (Oct1) and seems to correlate with the concerted translocation of ions discussed above. However, it may also reflect a ''relaxation'' of the KirBac filter structure (which was determined at a lower resolution) toward that seen in KcsA. There are also changes in the conformation of other carbonyls on a 1–10-ns timescale. For example, in Oct1 there are also changes in the CO ← → OC separation for G114 (data not shown).

Changes in the local conformation of the filter have also been seen in the POPC simulations. For example, in the PC2 simulation (Fig. 7) one of the peptide chains of the filter shows a fast (timescale ~0.8 ns) change in conformation and back again of the V111/G112 peptide bond such that the carbonyl oxygen moves toward and away from the center of the pore. Similar behavior has been seen in simulations of KcsA (Bernèche and Roux, 2000, 2001b; Shrivastava and Sansom, 2000; Shrivastava et al., 2002; Domene and Sansom, 2003) and of a homology model of Kir6.2 (Capener and Sansom, 2002) suggesting that such small (<0.1 nm) changes in backbone conformation may be an inherent property of K-channel filters.

The filter conformation at the V111/G112 peptide bond may be quantified in terms of the orientation of the CO

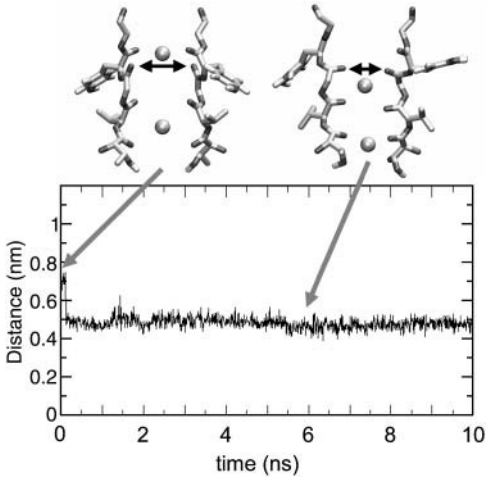


FIGURE 6 Flexibility of the selectivity filter during simulation Oct1. The distance between two opposing carbonyl oxygens of the G112 residues (as indicated by the double-headed arrows in the $t = 0$ and 6-ns snapshots shown above the graph) is shown as a function of time.

carbonyl vector relative to the center of the pore (see Table 2). It can be seen that, averaging across all four subunits in the four simulations with $K^+$ ions present (i.e., OCT1–PC2) the average angle is 21°. This is a little smaller (implying the COs point more directly toward the pore center) than in the KirBac x-ray structure (46°), but is very close to the equivalent angle (19°) in the KcsA (high [$K^+$]) x-ray structure. However, across the duration of the simulations the standard deviation of this angle is ~10°, indicative of a degree of flexibility. If we follow an individual V111 carbonyl flip, as in Fig. 7, then we see substantial changes in the angle with an angle of 150° at 1.15 ns, 42° at 1.30 ns, and 152° at 1.99 ns (corresponding to the CO pointing away from, toward, and away from the pore axis, respectively).

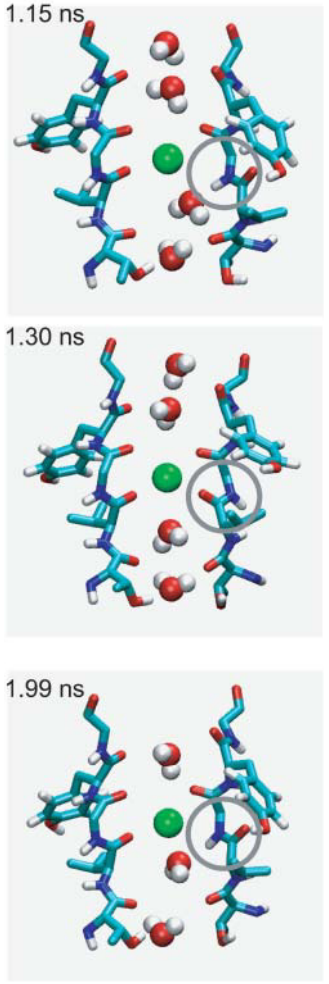


FIGURE 7 Three snapshots of the filter from the start of the PC2 simulation showing the ''flip'' in conformation of the V111/G112 peptide bond (as indicated by the *shaded circle*) of one of the four chains of the filter.

## Filter distortion

It has been shown for Kv channels that depletion of $K^+$ ions leads to a ''defunct'' channel with a presumed change in conformation in filter that enables a transient permeability to $Na^+$ ions (Khodakhah et al., 1998; Melishchuk et al., 1998; Loboda et al., 2001). Similar behavior is suggested to occur for KcsA (D. A. Doyle, personal communication). In simulations of KcsA, the absence of $K^+$ ions in the filter leads to filter distortion (Shrivastava and Sansom, 2000; Domene and Sansom, 2003; Holyoake et al., 2003). We therefore have run a simulation of KirBac, PC3, which omitted $K^+$ ions from the filter. The results of simulation PC3 indicate significant distortion of the filter. In particular the C$\alpha$ RMSD versus time of the filter residues is about twice that for a simulation (PC2) with $K^+$ ions present (Fig. 8). This corresponds to a much higher degree of filter distortion than the filter flexibility seen in simulations Oct1, Oct2, PC1, and PC2. This can be seen by measurement of the angle the V111 CO makes relative to the pore axis (see Table 2 and above). Thus, for simulations OCT1–PC2 the average value of this angle is 21°, corresponding to the carbonyl oxygen pointing toward the center of the pore. However, for three of the four carbonyls in simulations PC3 the angle is ~148°, corresponding to the oxygen pointing away from the pore throughout the simulation.

## Simulation comparisons

As discussed above, distortions of the KirBac filter are observed in simulations performed in the absence of $K^+$ ions. It is particularly informative to compare these distortions to those observed in other simulations and in some K-channel structures (Fig. 9). In particular it seems that in the absence of ions in the filter, both KirBac and KcsA undergo a distortion that flips a carbonyl (V111 in KirBac) and also widens the filter toward its extracellular end. This distortion is presumed to occur due to oxygen-oxygen

**TABLE 2 Filter flexibility at V111 in simulations**

| Angle between CO vector normal to pore axis (°) | | | | |
|---|---|---|---|---|
| X-ray | | 45.7 | | |
| Simulation | Subunit A | Subunit B | Subunit C | Subunit D |
| OCT1 | 11.4 (7.5) | 14.8 (9.3) | 12.3 (8.5) | 17.0 (12.0) |
| OCT2 | 29.6 (11.5) | 29.0 (14.6) | 35.6 (12.6) | 26.1 (11.7) |
| PC1 | 12.9 (9.0) | 9.4 (7.4) | 13.9 (8.9) | 15.2 (8.9) |
| PC2 | 25.8 (8.9) | 35.9 (14.4) | 23.8 (9.7) | 23.1 (9.1) |
| PC3 (no ions) | 19.8 (9.2) | 154.9 (12.2) | 133.1 (29.0) | 155.9 (10.4) |

The angle given is that formed in the *xy* plane between the CO vector and the normal to the *z* (pore) axis. Thus, if the carbonyl oxygen points directly towards the center of the pore, the angle is 0°. Angles given are mean ± SD across the duration of each simulation.

electrostatic repulsion in the absence of cations. Interestingly a similar distortion has been observed during simulations of a model of a low conductance mutant of Kir6.2 (Capener et al., 2003). We can quantify the distortion by measurement of the angle between the CO and the pore axis for V111 or the equivalent residue (see above and Table 3). It can be seen that in both the KirBac and KcsA simulations in the absence of ions, three of the four chains are distorted such that the valine carbonyl oxygen is directed away from the pore. For the Kir6.2 V127T mutant model, the equivalent isoleucine carbonyl oxygen is directed away from the pore for two of the four subunits. Comparison of the CO angle for all of the filter peptide residues for KcsA in its high and low [$K^+$] conformations shows that the biggest deviation is for V76.

This distortion, which is expected to functionally close the channel (as it leads to a narrowing of the channel and also directs the NH groups of Gly-112 toward the lumen, producing an electrostatic barrier to cation translocation) seems to correspond to a transition from $\alpha \rightarrow \beta$ conformation for V111 (or the equivalent valine in KcsA) and from $\alpha_L \rightarrow \beta$ for G112 (or the equivalent glycine in KcsA). Significantly a similar (if somewhat less pronounced) distortion occurs in the crystal structure of KcsA if grown in the presence of a low concentration of $K^+$ ions. Thus, it seems that the filter of KirBac and of other K channels is inherently sensitive to distortion and that a nonfunctional filter conformation may be induced either by a transient or prolonged absence of K+ ions from the filter or promoted by mutations in the vicinity of the filter. It seems likely that such distortions may underlie the phenomenon of ''fast'' (i.e., filter) gating in Kir channels and of C-type inactivation of Kv channels (see below for a more detailed discussion).

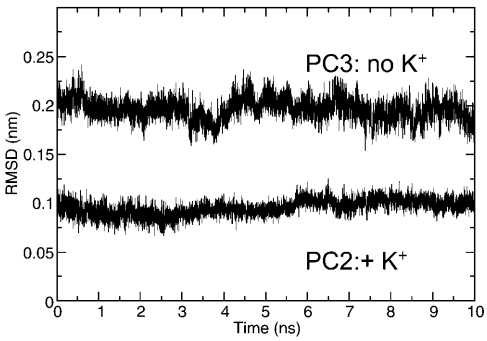


FIGURE 8 RMSD from the crystal structure of the C$\alpha$ atoms of the selectivity filter of KirBac simulations PC2 (with two $K^+$ ions in the filter) and PC3 (without $K^+$ ions).

## DISCUSSION

In this study we have focused our analysis on the conformational dynamics of the selectivity filter in relationship to ion permeation through KirBac channels. It is important to consider the timescale of the simulations relative to physiological timescales. The single channel conductance of KirBac is not known. However, in symmetrical 140 mM K solution, the conductances of Kir6.2 is 70 pS (Proks et al., 2001), of Kir1.1 is 40 pS, and of Kir2.1 is 30 pS (Choe et al., 2000) (also see Capener et al., 2003). So, if we assume a conductance of ~50 pS for KirBac, at a transmembrane voltage of 100 mV, this gives a current of 5 pA, corresponding to a mean ion passage time of ~30 ns. It is therefore reasonable to expect that 10-ns duration simulations will capture (some of) the events in the filter during ion permeation. Of course there will also be longer timescale processes that we have not observed. However, it is important to realize that simulations can make an important contribution to analysis of the conformational dynamics of the filter. In particular, the crystal structure is the temporal and spatial average of the channel molecules in the whole crystal and so individual correlations between, e.g., site occupancy and local filter conformation will be difficult to recover from experimental crystallographic data.

The main finding of the current study is that the KirBac filter exhibits a degree of flexibility. In the presence of ions within the filter, this flexibility corresponds to relative small (<0.1 nm) local changes in backbone conformation, which may correlate with the presence/absence of a $K^+$ ion at a given site. Similar flexibility has been seen in KcsA, and is likely to be associated with smoothing the energy landscape of ions within the filter (Bernèche and Roux, 2001a) so as to enable a high permeation rate. It is therefore of interest that mutations in the Kir selectivity filter backbone (e.g., Lu et al., 2001a) result in changes in single-channel conductance properties, as such mutations are likely to influence the local conformational dynamics of the filter.

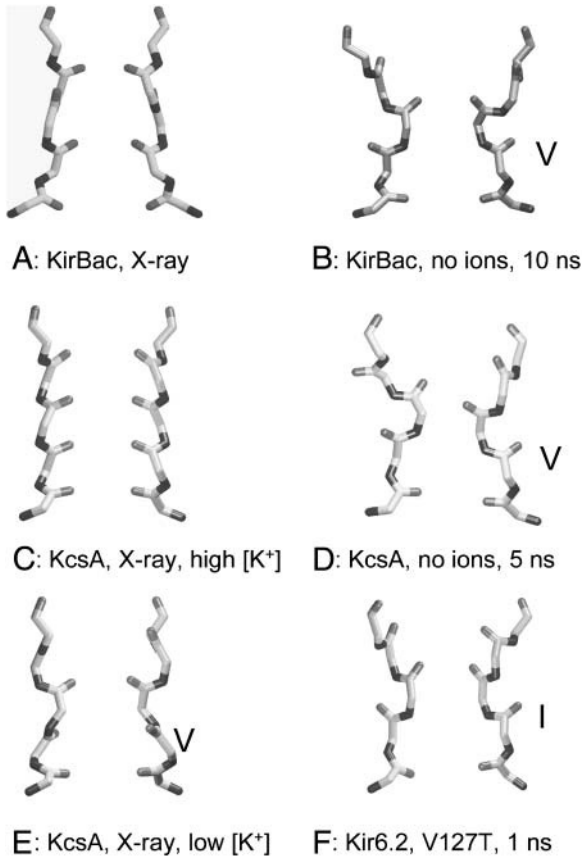


FIGURE 9 Structure of the selectivity filter in simulations and crystal structures compared. In each case the backbone of two subunits of the filter is shown. (*A*) KirBac x-ray structure; (*B*) KirBac, simulation PC3 (no $K^+$ ions) at the end (10 ns) of the simulation; (*C*) KcsA, crystallized in the presence of a high concentration of $K^+$ ions (PDB code 1k4c); (*D*) KcsA, from a simulation in which all $K^+$ ions have left the filter (Holyoake et al., 2003); (*E*) KcsA, crystallized in the presence of a low concentration of $K^+$ ions (PDB code 1k4d); and (*F*) a snapshot from a simulation of a model of a Kir6.2 mutant (Capener et al., 2003) that has impaired single-channel conductance. The flipped carbonyl of the valine residue of TVGYG is indicated with a V (this is replaced by an isoleucine, I131, in Kir6.2). (See Table 3 for analysis of the CO-pore normal angles for these residues.)

It is useful to consider experimental evidence in support of the notion of flexibility and/or distortion in the filter region of K channels, both Kir channels and others. This falls into two broad categories: crystallographic and electrophysiological. The crystallographic evidence is principally the difference between the low [$K^+$] and high [$K^+$] structures of KcsA (Zhou et al., 2001) where, as described above, the orientation of V76 changes. A similar change has been seen for low and high concentrations of thallium (Zhou and MacKinnon, 2003). Interestingly, in the latter study at intermediate concentrations of cation, the filter electron density was disordered, implying multiple conformations of this region within the same crystal. Some evidence of smaller degrees of flexibility is obtained by comparing, e.g., the valine CO angle for the KirBac and KcsA (high [$K^+$]) crystal structures

**TABLE 3 Filter flexibility in K channels compared**

| Structure | Angle between CO vector normal to pore axis (°) | | | | |
|---|---|---|---|---|---|
| KirBac, x-ray | | | 45.7 | | |
| KirBac, no ions, 10 ns | 15.9 | 162.7 | | 161.4 | 165.9 |
| KcsA, x-ray, high [$K^+$] | | | 19.2 | | |
| KcsA, no ions, 5 ns | 134.6 | 1.3 | | 135.2 | 166.7 |
| KcsA, x-ray, low [$K^+$] | | | 78.2 | | |
| Kir6.2, V127T, 1 ns | 178.3 | 20.5 | | 21.1 | 162.7 |

The structures are those shown in Fig. 9. The angle given is as in Table 2, i.e., that formed in the *xy* plane between the CO vector and the normal to the *z* (pore) axis. The angles are for residue V111 in KirBac, V76 in KcsA, and I131 in Kir6.2, V127T. For the structures taken from simulations, angles for each of the four subunits are given.

(Table 3). However, one must remember the difference in resolutions (3.7 vs. 2.0 Å) when making this comparison.

The electrophysiological evidence is inevitably less direct. For inward rectifier channels, a number of mutations in the filter region have been interpreted as indicative of filter flexibility/distortions. Thus, backbone mutations of Kir2.1 have been interpreted in terms of local changes in filter conformation related to ''fast gating'' (Lu et al., 2001a), as have side-chain mutations in the vicinity of the filter of Kir6.2 (Proks et al., 2001). Turning to Kv channels, changes in filter conformation have been implicated in C-type inactivation (Liu et al., 1996; Kiss et al., 1999) and in the formation of a defunct channel state in the absence of potassium ions (Loboda et al., 2001). However, the issue of timescales remains problematic. The simulation timescales are several orders of magnitude shorter than the electrophysiological timescales, and crystallographic data are temporal and spatial averages. Longer simulations and/or faster experimental measurements are needed.

The simulations of KirBac also suggest that the filter may undergo more pronounced distortions, with peptide bond flips, especially in the absence of $K^+$ ions. In this context it is also of interest that changes in the permeant ion (e.g., from $K^+$ to $Tl^+$; Lu et al., 2001b) can alter the mean open time of Kir2.1 channels, an effect that has been ascribed to ion-induced filter distortion. What is quite persuasive is the correlation between filter distortion observed in simulations of KirBac, KcsA, and homology models of Kir6.2 based on KcsA. Taken together, and in combination with the change in selectivity filter conformation induced in the KcsA crystal structure by a lowering of the $K^+$-ion concentration, these results provide a clear model of the likely conformational change in the selectivity filter of Kir channels that underlies gating at the selectivity filter (see also the discussion in Bichet et al., 2003).

Previous simulation studies, by us and by others (Bernèche and Roux, 2000, 2001b; Shrivastava and Sansom, 2000; Shrivastava et al., 2002; Domene and Sansom, 2003), have focused on such distortions in KcsA, or in KcsA-based homology models. The current study, based on simulations of an independent K-channel structure, supports the value of

multiple, comparative MD simulations to probe the generality, and hence likely biological significance, of simulation results. In a different study, we have demonstrated the value of comparative simulations in studying, e.g., conformational changes in glutamate receptors and related proteins (Arinaminpathy et al., 2002; Pang et al., 2003). It seems likely that comparisons between multiple MD simulations of related systems will become of increasing biological importance, suggesting a need for a database in which to store the results of simulation studies in an accessible form (cf. www.biosimgrid.org; Wu et al., 2003).

Our preliminary analysis, presented above, indicates that the slide helix of KirBac is capable of forming interactions with the headgroups of lipid molecules. Previous studies (Domene et al., 2003b) have indicated that extended (>10 ns) simulations of membrane proteins can provide details of lipid/protein interactions. It will therefore be of some interest o extend the current studies and analyze how lipid/protein interactions may be related to the conformational dynamics of the slide and M2 helix, particularly in the context of the suggested location of a phosphatidyinositol-4,5-*bis*-phosphate binding site close to the slide/M2 region in certain mammalian Kir channels (Bichet et al., 2003).

From a methodological perspective, we note that the current simulations have treated long-range electrostatic interactions via a particle mesh Ewald method (Darden et al., 1993; Essmann et al., 1995) as is current best practice (Patra et al., 2003). However, we note that there is an ongoing debate concerning possible artifacts arising from the use of such methods (Bostick and Berkowitz, 2003; Kastenholz and Hünenberger, 2004; Hünenberger and McCammon, 1999) and that periodicity artifacts have to be corrected in calculation of ion channel free-energy profiles (Allen et al., 2004). Given this, a more systematic study of the influence of simulation protocols on the outcome of ion channel simulations is needed. We are currently exploring the sensitivity of ion channel simulations to these and other simulation protocol details using KcsA as a test case (C. Domene and M. S. P. Sansom, unpublished data).

Finally, we note that the current studies provide only a first glimpse of the conformational dynamics of Kir channels. In particular, we need to establish a more global picture of the conformational changes possible in the molecule, and particularly of possible mechanisms of allosteric coupling between changes in the intracellular domain, the M2 (intracellular) gate, and the selectivity filter. This will be a challenge for the future, and will require careful correlation between computational and experimental data.

Our thanks to the Oxford Supercomputing Centre for computer time, and to all of our colleagues, especially Sundeep Deol, Declan Doyle, and Frances Ashcroft, for their continued interest in these studies.

This work was supported by grants from the Wellcome Trust and the Biotechnology and Biological Sciences Research Council (to M.S.P.S.) and the Royal Soc (to C.D.).

## REFERENCES

Allen, T. W., and S. H. Chung. 2001. Brownian dynamics study of an open-state KcsA potassium channel. *Biochim. Biophys. Acta.* 1515:83–91.

Allen, T. W., O. S. Andersen, and B. Roux. 2004. Energetics of ion conduction through the gramicidin channel. *Proc. Natl. Acad. Sci. USA.* 101:117–122.

Allen, T. W., A. Bliznyuk, A. P. Rendell, S. Kuyucak, and S. H. Chung. 2000. The potassium channel: structure, selectivity and diffusion. *J. Chem. Phys.* 112:8191–8204.

Allen, T. W., S. Kuyucak, and S. H. Chung. 1999. Molecular dynamics study of the KcsA potassium channel. *Biophys. J.* 77:2502–2516.

Åqvist, J. 1990. Ion water interaction potentials derived from free-energy perturbation simulations. *J. Phys. Chem.* 94:8021–8024.

Åqvist, J., and V. Luzhkov. 2000. Ion permeation mechanism of the potassium channel. *Nature.* 404:881–884.

Arinaminpathy, Y., M. S. P. Sansom, and P. C. Biggin. 2002. Molecular dynamics simulations of the ligand binding domain of the ionotropic glutamate receptor, GluR2. *Biophys. J.* 82:676–683.

Berendsen, H. J. C., J. P. M. Postma, W. F. van Gunsteren, and J. Hermans. 1981. Intermolecular Forces. Reidel, Dordrecht, The Netherlands.

Berger, O., O. Edholm, and F. Jahnig. 1997. Molecular dynamics simulations of a fluid bilayer of dipalmitoylphosphatidycholine at full hydration, constant pressure, and constant temperature. *Biophys. J.* 72: 2002–2013.

Bernèche, S., and B. Roux. 2000. Molecular dynamics of the KcsA $K^+$ channel in a bilayer membrane. *Biophys. J.* 78:2900–2917.

Bernèche, S., and B. Roux. 2001a. Energetics of ion conduction through the $K^+$ channel. *Nature.* 414:73–77.

Bernèche, S., and B. Roux. 2001b. Mechanism of ions permeation in the KcsA potassium channel. *Biophys. J.* 80:175a.

Bernèche, S., and B. Roux. 2003. A microscopic view of ion conduction through the $K^+$ channel. *Proc. Natl. Acad. Sci. USA.* 100:8644–8648.

Bichet, D., F. A. Haass, and L. Y. Jan. 2003. Merging functional studies with structures of inward-rectifier K+ channels. *Nat. Rev. Neurosci.* 4:957–967.

Biggin, P. C., G. R. Smith, I. H. Shrivastava, S. Choe, and M. S. P. Sansom. 2001. Potassium and sodium ions in a potassium channel studied by molecular dynamics simulations. *Biochim. Biophys. Acta.* 1510:1–9.

Bostick, D. L., and M. L. Berkowitz. 2003. The implementation of slab geometry for membrane-channel molecular dynamics simulations. *Biophys. J.* 85:97–107.

Capener, C. E., and M. S. P. Sansom. 2002. MD simulations of a K channel model: sensitivity to changes in ions, waters and membrane environment. *J. Phys. Chem. B.* 106:4543–4551.

Capener, C. E., P. Proks, F. M. Ashcroft, and M. S. P. Sansom. 2003. Filter flexibility in a mammalian K channel: models and simulations of Kir6.2 mutants. *Biophys. J.* 84:2345–2356.

Capener, C. E., I. H. Shrivastava, K. M. Ranatunga, L. R. Forrest, G. R. Smith, and M. S. P. Sansom. 2000. Homology modeling and molecular dynamics simulation studies of an inward rectifier potassium channel. *Biophys. J.* 78:2929–2942.

Choe, H., H. Sackin, and L. G. Palmer. 2000. Permeation properties of inward-rectifier potassium channels and their molecular determinants. *J. Gen. Physiol.* 115:391–404.

Chung, S. H., and S. Kuyucak. 2002. Ion channels: recent progress and prospects. *Eur. Biophys. J.* 31:283–293.

Compoint, M., P. Carloni, C. Ramseyer, and C. Girardet. 2004. Molecular dynamics study of the KcsA channel at 2.0-Å resolution: stability and concerted motions within the pore. *Biochim. Biophys. Acta.* 1661:26–39.

Darden, T., D. York, and L. Pedersen. 1993. Particle mesh Ewald: an N.log(N) method for Ewald sums in large systems. *J. Chem. Phys.* 98: 10089–10092.

de Groot, B. L., and H. Grubmuller. 2001. Water permeation across biological membranes: mechanism and dynamics of aquaporin-1 and GlpF. *Science*. 294:2353–2357.

Domene, C., and M. S. P. Sansom. 2003. A potassium channel, ions and water: simulation studies based on the high resolution x-ray structure of KcsA. *Biophys. J*. 85:2787–2800.

Domene, C., P. Bond, and M. S. P. Sansom. 2003a. Membrane protein simulation: ion channels and bacterial outer membrane proteins. *Adv. Protein Chem*. 66:159–193.

Domene, C., P. J. Bond, S. S. Deol, and M. S. P. Sansom. 2003b. Lipid-protein interactions and the membrane/water interfacial region. *J. Am. Chem. Soc*. 125:14966–14967.

Doyle, D. A., J. M. Cabral, R. A. Pfuetzner, A. Kuo, J. M. Gulbis, S. L. Cohen, B. T. Cahit, and R. MacKinnon. 1998. The structure of the potassium channel: molecular basis of $K^+$ conduction and selectivity. *Science*. 280:69–77.

Essmann, U., L. Perera, M. L. Berkowitz, T. Darden, H. Lee, and L. G. Pedersen. 1995. A smooth particle mesh Ewald method. *J. Chem. Phys*. 103:8577–8593.

Giorgetti, A., and P. Carloni. 2003. Molecular modeling of ion channels: structural predictions. *Curr. Opin. Chem. Biol*. 7:150–156.

Guidoni, L., and P. Carloni. 2002. Potassium permeation through the KcsA channel: a density functional study. *Biochim. Biophys. Acta*. 1563:1–6.

Guidoni, L., V. Torre, and P. Carloni. 1999. Potassium and sodium binding in the outer mouth of the $K^+$ channel. *Biochemistry*. 38:8599–8604.

Guidoni, L., V. Torre, and P. Carloni. 2000. Water and potassium dynamics in the KcsA $K^+$ channel. *FEBS Lett*. 477:37–42.

Hess, B., H. Bekker, H. J. C. Berendsen, and J. G. E. M. Fraaije. 1997. LINCS: a linear constraint solver for molecular simulations. *J. Comput. Chem*. 18:1463–1472.

Holyoake, J., C. Domene, J. N. Bright, and M. S. P. Sansom. 2003. KcsA closed and open: modelling and simulation studies. *Eur. Biophys. J*. [Epub ahead of print].

Hoover, W. G. 1985. Canonical dynamics: equilibrium phase-space distributions. *Phys. Rev. A*. 31:1695–1697.

Humphrey, W., A. Dalke, and K. Schulten. 1996. VMD: visual molecular dynamics. *J. Mol. Graph*. 14:33–38.

Hünenberger, P. H., and J. A. McCammon. 1999. Effect of artificial periodicity in simulations of biomolecules under Ewald boundary conditions: a continuum electrostatics study. *Biophys. Chem*. 78:69–88.

Jensen, M. O., E. Tajkhorshid, and K. Schulten. 2001. The mechanism of glycerol conduction in aquaglyceroporins. *Structure*. 9:1083–1093.

Jiang, Y., A. Lee, J. Chen, M. Cadene, B. T. Chait, and R. MacKinnon. 2002a. Crystal structure and mechanism of a calcium-gated potassium channel. *Nature*. 417:515–522.

Jiang, Y., A. Lee, J. Chen, M. Cadene, B. T. Chait, and R. MacKinnon. 2002b. The open pore conformation of potassium channels. *Nature*. 417:523–526.

Jiang, Y., A. Lee, J. Chen, V. Ruta, M. Cadene, B. T. Chait, and R. Mackinnon. 2003. X-ray structure of a voltage-dependent $K^+$ channel. *Nature*. 423:33–41.

Jordan, P. 2000. Ionic energetics in narrow channels. *In* Proceedins of the IMA Workshop on Membrane Transport and Renal Physiology. H. Layton, editor. Springer-Verlag, New York.

Kabsch, W., and C. Sander. 1983. Dictionary of protein secondary structure: pattern-recognition of hydrogen-bonded and geometrical features. *Biopolymers*. 22:2577–2637.

Kastenholz, M. A., and P. H. Hünenberger. 2004. Influence of artificial periodicity and ionic strength in molecular dynamics simulations of charged biomolecules employing lattice-sum methods. *J. Phys. Chem. B*. 108:774–788.

Khodakhah, K., A. Melishchuk, and C. M. Armstrong. 1998. Killing K channels with $TEA^+$. *Proc. Natl. Acad. Sci. USA*. 94:13335–13338.

Killian, J. A. 2003. Synthetic peptides as models for intrinsic membrane proteins. *FEBS Lett*. 555:134–138.

Killian, J. A., and G. von Heijne. 2000. How proteins adapt to a membrane-water interface. *Trends Biochem. Sci*. 25:429–434.

Kiss, L., J. LoTurco, and S. J. Korn. 1999. Contribution of the selectivity filter to inactivation in potassium channels. *Biophys. J*. 76:253–263.

Kuo, A., J. M. Gulbis, J. F. Antcliff, T. Rahman, E. D. Lowe, J. Zimmer, J. Cuthbertson, F. M. Ashcroft, T. Ezaki, and D. A. Doyle. 2003. Crystal structure of the potassium channel KirBac1.1 in the closed state. *Science*. 330:1921–1926.

Lindahl, E., B. Hess, and D. van der Spoel. 2001. GROMACS 3.0: a package for molecular simulation and trajectory analysis. *J. Mol. Model*. 7:306–317.

Liu, Y., M. E. Jurman, and G. Yellen. 1996. Dynamic rearrangement of the outer mouth of a $K^+$ channel during gating. *Neuron*. 16:859–867.

Loboda, A., A. Melishchuk, and C. Armstrong. 2001. Dilated and defunct K channels in the absence of $K^+$. *Biophys. J*. 80:2704–2714.

Lu, T., A. Y. Ting, J. Mainland, L. Y. Jan, P. G. Schultz, and J. Yang. 2001a. Probing ion permeation and gating in a K+ channel with backbone mutations in the selectivity filter. *Nat. Neurosci*. 4:239–246.

Lu, T., L. Wu, J. Xiao, and J. Yang. 2001b. Permeant ion-dependent changes in gating of Kir2.1 inward rectifier potassium channels. *J. Gen. Physiol*. 118:509–521.

Luzhkov, V. B., and J. Åqvist. 2000. A computational study of ion binding and protonation states in the KcsA potassium channel. *Biochim. Biophys. Acta*. 1481:360–370.

Luzhkov, V. B., and J. Åqvist. 2001. Mechanisms of tetraethylammonium ion block in the KcsA potassium channel. *FEBS Lett*. 495:191–196.

Mackinnon, R. 2003. Potassium channels. *FEBS Lett*. 555:62–65.

Marrink, S. J., O. Berger, D. P. Tieleman, and F. Jahnig. 1998. Adhesion forces of lipids in a phospholipid membrane studied by molecular dynamics simulations. *Biophys. J*. 74:931–943.

Mashl, R. J., Y. Z. Tang, J. Schnitzer, and E. Jakobsson. 2001. Hierarchical approach to predicting permeation in ion channels. *Biophys. J*. 81:2473–2483.

Melishchuk, A., A. Loboda, and C. M. Armstrong. 1998. Loss of *Shaker* K channel conductance in 0 $K^+$ solutions: role of the voltage sensor. *Biophys. J*. 75:1828–1835.

Morais-Cabral, J. H., Y. Zhou, and R. MacKinnon. 2001. Energetic optimization of ion conduction by the $K^+$ selectvity filter. *Nature*. 414:37–42.

Nichols, C. G., and A. N. Lopatin. 1997. Inward rectifier potassium channels. *Annu. Rev. Physiol*. 59:171–191.

Nishida, M., and R. MacKinnon. 2002. Structural basis of inward rectification: cytoplasmic pore of the G protein-gated inward rectifier GIRK1 at 1.8 Å resolution. *Cell*. 111:957–965.

Pang, A., Y. Arinaminpathy, M. S. P. Sansom, and P. C. Biggin. 2003. Interdomain dynamics and ligand binding: molecular dynamics simulations of glutamine binding protein. *FEBS Lett*. 550:168–174.

Patra, M., M. Karttunen, M. T. Hyvönen, E. Falck, P. Lindqvist, and I. Vattulainen. 2003. Molecular dynamics simulations of lipid bilayers: major artifacts due to truncating electrostatic interactions. *Biophys. J*. 84:3636–3645.

Proks, P., C. E. Capener, P. Jones, and F. Ashcroft. 2001. Mutations within the P-loop of Kir6.2 modulate the intraburst kinetics of the ATP-sensitive potassium channel. *J. Gen. Physiol*. 118:341–353.

Ranatunga, K. M., I. H. Shrivastava, G. R. Smith, and M. S. P. Sansom. 2001a. Side-chain ionization states in a potassium channel. *Biophys. J*. 80:1210–1219.

Ranatunga, K. M., G. R. Smith, R. J. Law, and M. S. P. Sansom. 2001b. Electrostatics and molecular dynamics of a homology model of the *Shaker* $K^+$ channel pore. *Eur. Biophys. J*. 30:295–303.

Reimann, F., and F. M. Ashcroft. 1999. Inwardly rectifying potassium channels. *Curr. Opin. Cell Biol*. 11:503–508.

Roux, B. 2002. Theoretical and computational models of ion channels. *Curr. Opin. Struct. Biol*. 12:182–189.

Roux, B., S. Bernèche, and W. Im. 2000. Ion channels, permeation and electrostatics: insight into the function of KcsA. *Biochemistry*. 39:13295–13306.

Sansom, M. S. P., I. H. Shrivastava, J. N. Bright, J. Tate, C. E. Capener, and P. C. Biggin. 2002. Potassium channels: structures, models, simulations. *Biochim. Biophys. Acta*. 1565:294–307.

Sansom, M. S. P., I. H. Shrivastava, K. M. Ranatunga, and G. R. Smith. 2000. Simulations of ion channels: watching ions and water move. *Trends Biochem. Sci*. 25:368–374.

Shrivastava, I. H., and M. S. P. Sansom. 2000. Simulations of ion permeation through a potassium channel: molecular dynamics of KcsA in a phospholipid bilayer. *Biophys. J*. 78:557–570.

Shrivastava, I. H., and M. S. P. Sansom. 2002. Molecular dynamics simulations and KcsA channel gating. *Eur. Biophys. J*. 31:207–216.

Shrivastava, I. H., D. P. Tieleman, P. C. Biggin, and M. S. P. Sansom. 2002. $K^+$ vs. $Na^+$ ions in a K channel selectivity filter: a simulation study. *Biophys. J*. 83:633–645.

Tajkhorshid, E., P. Nollert, M. O. Jensen, L. J. W. Miercke, J. O'Connell, R. M. Stroud, and K. Schulten. 2002. Control of the selectivity of the aquaporin water channel family by global orientational tuning. *Science*. 296:525–530.

Tieleman, D. P., H. J. C. Berendsen, and M. S. P. Sansom. 2001a. Voltage-dependent insertion of alamethicin at phospholipid/water and octane/water interfaces. *Biophys. J*. 80:331–346.

Tieleman, D. P., P. C. Biggin, G. R. Smith, and M. S. P. Sansom. 2001b. Simulation approaches to ion channel structure-function relationships. *Qt. Rev. Biophys*. 34:473–561.

van Gunsteren, W. F., and H. J. C. Berendsen. 1987. Gromos-87 Manual. Biomos BV, Groningen, The Netherlands.

Vriend, G. 1990. WhatIf: a molecular modeling and drug design program. *J. Mol. Graph*. 8:52–56.

Wu, B., K. Tai, S. Murdock, M. G. Ng, S. Johnston, H. Fangohr, P. Jeffreys, J. Cox, J. Essex, and M. S. P. Sansom. 2003. BioSimGRID: a distributed database for biomolecular simulations. *In* Proc. UK e-Science All Hands Meeting 2003, Nottingham, UK. 412–419.

Yau, W. M., W. C. Wimley, K. Gawrisch, and S. H. White. 1998. The preference of tryptophan for membrane interfaces. *Biochemistry*. 37:14713–14718.

Yellen, G. 2002. The voltage-gated potassium channels and their relatives. *Nature*. 419:35–42.

Zhou, Y., and R. MacKinnon. 2003. The occupancy of ions in the $K^+$ selectivity filter: charge balance and coupling of ion binding to a protein conformational change underlie high conduction rates. *J. Mol. Biol*. 333:965–975.

Zhou, Y., J. H. Morais-Cabral, A. Kaufman, and R. MacKinnon. 2001. Chemistry of ion coordination and hydration revealed by a $K^+$ channel-Fab complex at 2.0 Å resolution. *Nature*. 414:43–48.

Zhu, F. Q., E. Tajkhorshid, and K. Schulten. 2001. Molecular dynamics study of aquaporin-1 water channel in a lipid bilayer. *FEBS Lett*. 504:212–218.